Chemical Research in Toxicology

Article

pubs.acs.org/crt

DNA Polymerase β Gap-Filling Translesion DNA Synthesis

Parvathi Chary,[†] William A. Beard,[‡] Samuel H. Wilson,[‡] and R. Stephen Lloyd*[,†]

[†]Center for Research on Occupational and Environmental Toxicology (CROET), Oregon Health & Science University, 3181 SW Sam Jackson Park Road, Portland, Oregon 97239-3098, United States

[‡]Laboratory of Structural Biology, National Institute of Environmental Sciences, National Institutes of Health, P.O. Box 12233, Research Triangle Park, North Carolina 27709, United States

ABSTRACT: Although the primary function of DNA polymerase (pol) β is associated with gap-filling DNA synthesis as part of the DNA base excision repair pathway, translesion synthesis activity has also been described. To further understand the potential role of pol β-catalyzed translesion DNA synthesis (TLS) and the structure−function relationships of specific residues in pol β, wild-type and selected mutants of pol β were used in TLS assays with DNA substrates containing bulky polycyclic aromatic hydrocarbon-adducted oligonucleotides. Stereospecific (+) and (−)-*anti-trans*-($C_{10}S$ and $C_{10}R$) benzo[*a*]pyrene-7,8- dihydrodiol-9-10-epoxide (BPDE) adducts were covalently attached to both the N^6-adenine and N^2-guanine in the major and minor grooves, respectively. For all substrates tested, the presence of the BPDE adducts greatly decreased the efficiency of nucleotide incorporation opposite the lesion, and the stereochemistry of the adducts also further modulated the efficiency of the insertion step, such that lesions which were oriented in the 3′ direction relative to the approaching polymerase were considerably more blocking than those oriented in the 5′ direction. In the absence of a downstream DNA strand, the extension step beyond the adduct was extremely inefficient, relative to a dinucleotide gap-filling reaction, such that in the presence of the downstream DNA, dinucleotide incorporation was strongly favored. In general, analyses of the TLS activities of four pol β mutants revealed similar overall properties, but wild-type pol β exhibited more than 50-fold greater extension and bypass of the $C_{10}S$-dA adducts as compared to a low fidelity mutant R283K expected to interact with the templating base. Replication bypass investigations were further extended to include analyses of HIV-1 reverse transcriptase, and these studies revealed patterns of inhibition very similar to that observed for pol β.

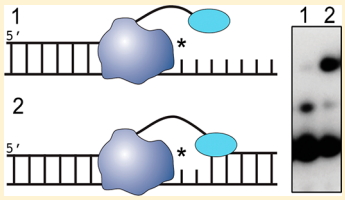

INTRODUCTION

DNA polymerase (pol) β is the smallest eukaryotic polymerase (39 kDa) belonging to the X-family of DNA polymerases and has been extensively characterized biologically, computationally, kinetically, and structurally.[1] It is composed of two domains that together function to coordinate the DNA synthesis steps in base excision repair. The amino-terminal 8 kDa domain includes lyase activity that removes the 5′-deoxyribose phosphate generated after incision by apurinic/apyrimidinic endonuclease during the repair of simple base lesions.[2,3] The lyase domain recognizes the 5′-phosphate in DNA gaps thereby targeting the polymerase for gap-filling DNA synthesis.[4] The nucleotidyl transferase activity of pol β resides in the 31 kDa polymerase domain. A helix−hairpin−helix (HhH) structural motif is found in each domain and interacts with the DNA backbone in a nonsequence-dependent manner on opposite sides of gapped DNA. The HhH motif is conserved in other members of the X-family DNA polymerases and is believed to facilitate DNA gap binding.[5]

Although the primary cellular role of pol β is to provide lyase and nucleotidyl transferase activities during base excision repair of simple DNA base lesions, pol β has also been implicated in the replication bypass of a variety of bulky DNA lesions. Overexpression of pol β can result in decreased sensitivity to agents that generate bulky DNA adducts such as cisplatin[6] or UV radiation.[7] *In vitro* assays demonstrate the ability of pol β to bypass UV,[7] benzo[*c*] phenanthrene diolepoxides,[8] and cisplatin-induced DNA lesions.[9,10] Translesion synthesis past platinum-DNA adducts was greater with gapped DNA templates than with single-stranded DNA templates.[10] Pol β can bypass abasic sites[11] and 8-oxo-deoxyguanine[12] in short DNA gaps by utilizing the downstream templating base for coding and is consistent with its low deletion frameshift fidelity in gapped DNA.[13] This observation suggests that lesion bypass might occur by employing the downstream templating base. In contrast, structures of pol β with active site mismatches indicate that the incorrect templating base is positioned upstream of the coding template base pocket creating a pseudoabasic site (i.e., coding potential of the templating pocket is lost).[14] Accordingly, an alternate mechanism for the bypass of a bulky lesion is to remove the modified nucleotide from the templating pocket through template strand upstream translocation or alternatively, expelling the lesion to an extra-helical position. Finally, auxiliary replication proteins, replication protein A and proliferating cell nuclear antigen, have also been reported to influence the efficiency and fidelity of translesion DNA synthesis past thymine glycol[15] and 8-oxo-deoxyguanine in gapped DNA.[16]

Furthermore, persistent bulky adducts in DNA block the progression of replicative DNA polymerases[17,18] and RNA polymerase II.[19] Among these bulky DNA adducts are polycyclic aromatic hydrocarbons such as benzo[*a*]pyrene. These are

Received: August 30, 2012
Published: November 2, 2012

dx.doi.org/10.1021/tx300368f | *Chem. Res. Toxicol.* 2012, 25, 2744−2754

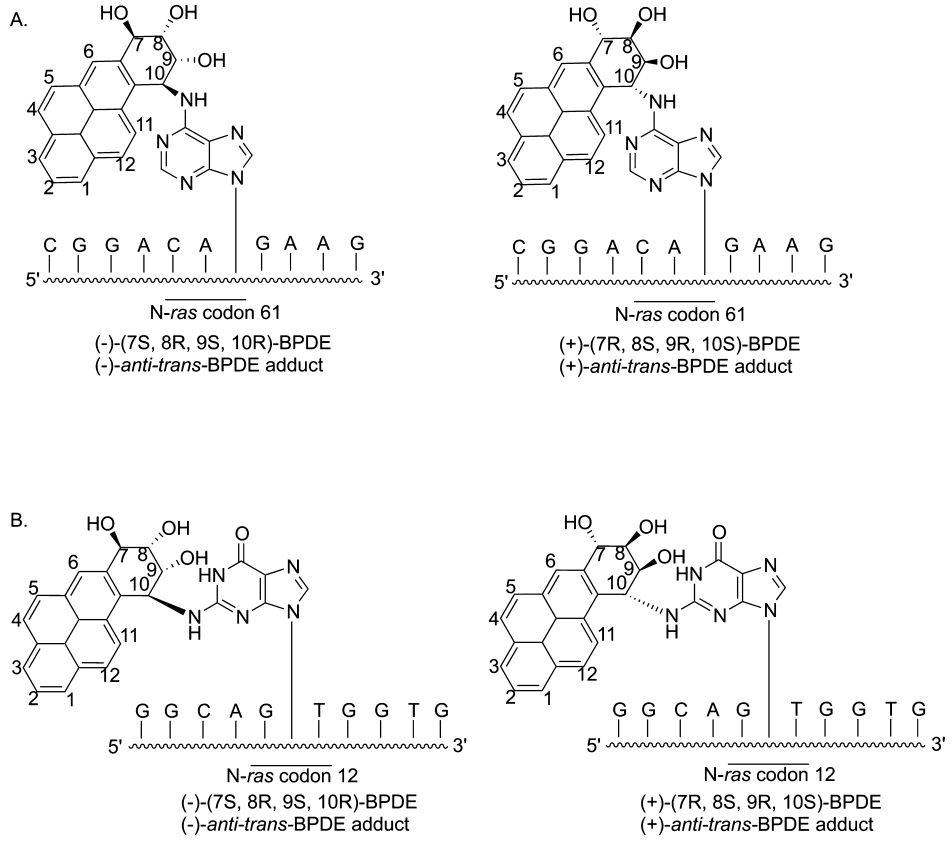

Figure 1. Structures of BPDE adducts. (A) Sequence and structure of the (−) and (+) *anti-trans*-BPDE adducts covalently attached to N^6 of adenine in the N-*ras* codon 61[3] on an 11-mer oligonucleotide. (B) Sequence and structure of the (−) and (+) *anti-trans*-BPDE adducts covalently attached to N^2 of guanine in the N-*ras* codon 12[2] in an 11-mer oligonucleotide.

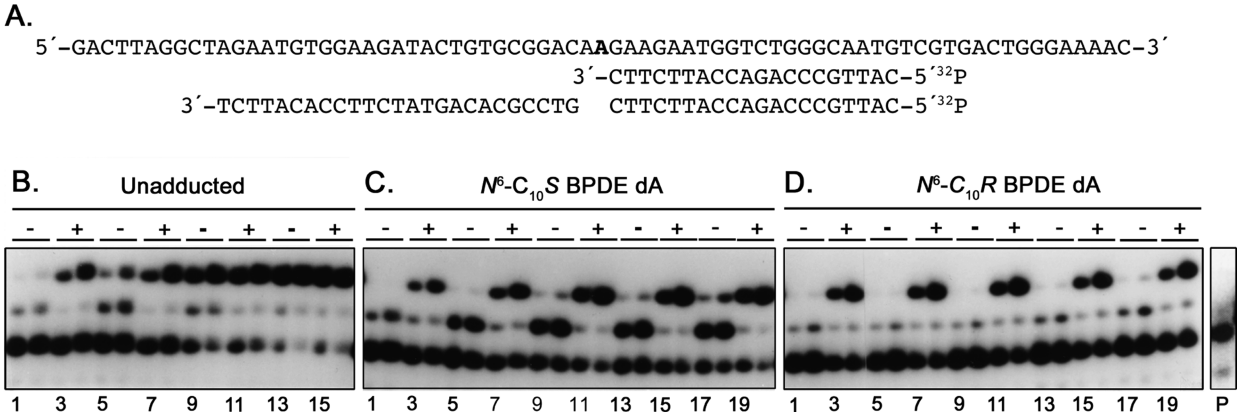

Figure 2. DNA pol β catalyzed DNA synthesis modulated by gapped DNA and a major-groove BPDE-adduct. (A) Schematic of DNA substrates for DNA synthesis reactions. The bold **A** indicates the position of the unadducted, $C_{10}S$ BPDE-dA or $C_{10}R$ BPDE-dA. The radio-labeled primer strand is indicated by the 5′-^{32}P label. (B) DNA synthesis reactions using an unadducted template without (−) or with (+) a downstream unlabeled oligonucleotide strand. Odd and even numbered lanes represent 5 and 15 min reactions, respectively. Lanes 1−4, 5−8, 9−12, and 13−16 include pol β (10 fmol) with 0.1, 0.2, 0.5, and 1 μM dTTP, respectively. (C) DNA synthesis reactions using the $C_{10}S$ BPDE-dA adducted template without (−) or with (+) a downstream unlabeled oligonucleotide strand. Odd and even numbered lanes represent 5 and 15 min reactions, respectively. Lanes 1−4, 5−8, 9−12, 13−16, and 17−20 include pol β (10 fmol) with 100, 200, 500, 1000, and 1500 μM dTTP, respectively. (D) DNA synthesis reactions using the $C_{10}R$ BPDE-dA adducted template without (−) or with (+) a downstream unlabeled oligonucleotide strand. Odd and even numbered lanes represent 5 and 15 min reactions, respectively. Lanes 1−4, 5−8, 9−12, 13−16, and 17−20 include pol β (10 fmol) with 2.25, 2.5, 2.75, 3, and 3.25 mM dTTP, respectively.

tumorigenic in animal models and are suspected human carcinogens. Benzo[*a*]pyrene is metabolically activated to 7,8-dihydrodiol-9,10-epoxides (BPDE) that can damage DNA by forming adducts, mainly at the exocyclic 2- and 6-amino groups of guanine and adenine, respectively.[20]

Our earlier studies of pol β replication with various stereospecific BPDE-adducted templates were performed with nongapped DNA where synthesis was distributive (i.e., polymerase would dissociate from the DNA substrate after every nucleotide insertion). In this situation, long incubation times

dx.doi.org/10.1021/tx300368f | *Chem. Res. Toxicol.* 2012, 25, 2744−2754

resulted in products that primarily terminated synthesis prior to or opposite the lesion.[21] The present study circumvents the replication block of these bulky lesions by placing the lesion in the single-stranded template strand of short-gapped DNA. The stereospecific BPDE-adduct was positioned either in the DNA major groove (N^6 adenine adduct in the N-*ras* codon 61[3], CA<u>A</u>) or the minor groove (N^2 guanine adduct in the N-*ras* codon 12[2], G<u>G</u>T). In addition, several pol β mutants were examined that alter DNA minor groove contacts to probe the effect on lesion bypass.

EXPERIMENTAL PROCEDURES

Materials. T4 polynucleotide kinase and T4 DNA ligase were obtained from New England BioLabs Inc. (Ipswich, MA). Human pol β and four mutants (K234A, Y271A, N279A, and R283K) and HIV-1 reverse transcriptase (RT) were expressed in *Escherichia coli* as previously described.[22,23] Oligonucleotides (11-mers) containing site- and stereospecific benzo[*a*]pyrene diolepoxide adducts in either of two different stereochemical orientations (−)-(7*S*,8*R*,9*S*,10*R*)-BPDE-dA or (+)-(7*R*,8*S*,9*R*,10*S*)-BPDE-dA (Figure 1A) and (−)-(7*S*,8*R*,9*S*,10*R*)-BPDE-dG or (+)-(7*R*,8*S*,9*R*,10*S*)-BPDE-dG (Figure 1B) were gifts from Drs. Thomas and Constance Harris, Department of Chemistry, Vanderbilt University. These were prepared as described previously using a postoligomerization strategy.[24,25] All dNTPs were purchased from Pharmacia (Piscataway, NJ). Oligonucleotides were 5′-end-labeled with [γ^{32}P] ATP (3000 Ci/mMol) (Dupont NEN, Boston, MA).

Construction and Purification of Adducted Templates. A control unadducted 73-mer template DNA and BPDE-adducted 11-mers ($C_{10}S$ or $C_{10}R$ on N^6 adenine or N^2 guanine) were purified by electrophoretic separation through 10% and 15% polyacrylamide sequencing gels, respectively. These were then incorporated into 73-mers using a 46-mer DNA scaffold, in which the 11-mer adducted DNAs were ligated with two additional oligonucleotides (30- and 32-mers) at the 5′- and 3′-termini of the 11-mer, respectively. The 73-mer adducted templates and primers were purified by electrophoresis through 10% polyacrylamide denaturing gels containing 8 M urea. The appropriate bands were excised from the gel, crushed, and suspended in water. To remove urea, the oligonucleotides were ethanol precipitated and washed six to eight times with 70% alcohol. The adducted and control templates were resuspended in water and concentrations calculated from their absorbance at 260 nm. Figures 2A and 4A illustrate the constructed DNA substrates where the upstream and downstream oligonucleotides are 5′-phoshphorylated with [γ^{32}P] ATP or unlabeled ATP, respectively.

Primer Extension and Gap-Filling DNA Synthesis by Wild-Type and Mutant Pol β. Oligonucleotide primers were labeled with [γ^{32}P] ATP by T4 polynucleotide kinase following the manufacture's protocol. Gap-filling DNA synthesis with wild-type pol β and mutants were carried out on substrates created by annealing oligonucleotides (template/labeled primer/downstream oligodeoxynucleotide) in a ratio of 5 (250 fM):1 (50 fM):3 (150 fM). The annealing mixtures were incubated at 65 °C for 3 min and cooled gradually to 30 °C in 70 min. For primer extension reactions in the absence of a downstream oligonucleotide, the template/labeled primer was 5 (250 fM):1 (50 fM). Kinase reactions were performed using 12.5 pmoles of the primer oligonucleotide in a final buffer containing 70 mM Tris-HCl (pH 7.6), 10 mM $MgCl_2$, 5 mM dithiothreitol, 10 mM β mercaptoethanol, 50 pmol [γ^{32}P] ATP, and 20 units of T4 polynucleotide kinase in a total reaction volume of 25 μL. The reaction mixtures were incubated at 37 °C for 70 min, after which the kinase was inactivated by heating to 65 °C for 20 min.

Polymerization reactions were initiated by the addition of wild-type pol β (10 fmol) or the mutant enzymes to the above mixture, and incubated at 37 °C for 5 or 15 min. Reactions were terminated by the addition of an equal volume of 95% formamide, 20 mM EDTA, 0.05% bromphenol blue, and 0.05% xylene cyanol. Prior to loading on the sequencing gel, the above mixtures were heated at 65 °C for 2 min, prior to loading 2 μL of each samples. DNAs were separated with 15% denaturing polyacrylamide sequencing gels and the bands quantified by PhosphorImager analyses. All reactions were carried out a minimum of 3 times, and the values reported are an average of those data.

Calculations of Catalytic Efficiencies of dNTP Incorporation, Insertion Efficiency, and Discrimination Factor. Incorporation rates of dNTPs were found to be linearly dependent over a range of dNTP concentrations up to 3 mM. The kinetics of primer extension at a particular enzyme concentration represents k_{cat}/K_m. Regression analyses of the plot k_{cat}/K_m versus dNTP concentration gave best fits to the data with the slope defining the catalytic efficiency k_{cat}/K_m (M/min) of the incorporation of a specific nucleotide on a particular adducted or control DNA template. The insertion efficiency allows for comparison between the incorporation of a specific nucleotide opposite the adducted sites and nucleotide addition at the control site. Consequently, the catalytic efficiency values corresponding to the control template were normalized to 1. Since each polymerase had different insertion efficiency values for a specific nucleotide and adducted template, the polymerase with the lowest insertion efficiency value was calculated and normalized to the value of 1. The discrimination factor compares the catalytic efficiency of wrong versus right nucleotide (dTTP opposite N^6 adenine and dCTP opposite N^2 guanine) incorporation opposite control or $C_{10}S$ or $C_{10}R$ adducted sites, having normalized the dTTP or dCTP values for a particular template to 1. Steady-state kinetic parameters were determined by fitting the rate data to the Michaelis equation by nonlinear regression analysis. When nucleotide insertion was poor (i.e., opposite an adduct), catalytic efficiencies were estimated from the linear portion ($S \ll K_m$) of a Michaelis curve where $k_{obs} \sim (k_{cat}/K_m)[S]$.

For the calculation of the bypass efficiency, it was assumed that all primers were hybridized. This was empirically established by demonstrating that under conditions of excess polymerase and dNTPs, >95% of the primers could be extended (data not shown). These data are in agreement with the experimental design in which the amount of template strand was in greater excess over primer (500%). The bypass efficiency is not a percentage of bypass but a calculation that takes into account the extent to which the reaction has progressed with any incorporation either opposite the lesion alone or insertion and extension of the primer. The extent of primer utilized was assumed to be random throughout the total population of DNA molecules and is given by the 0th term of the Poisson distribution (primers that have not been extended) and calculated as the −ln of the mass fraction of the unextended primer. This calculation takes into account all the possible lengths of the DNA molecules (no extension, and 1 and 2 nucleotides incorporated). By determining the 0th term of the Poisson distribution, differences in the relative efficiencies of primer utilization were accounted for by this calculation. This value was then multiplied by the percent of DNA molecules that have been extended by 2 nucleotides. Since the 0th term of the Poisson distribution takes into account all possible DNA lengths, and the experimental design was to assess the role that the downstream primer plays in increasing the efficiency of the second nucleotide incorporation; the product of these two values captures the change in the extension efficiencies based on the different DNA substrates.

RESULTS

Experimental Design. It has been previously established that the DNA synthesis activity and processivity of pol β was significantly increased when the substrate DNA was designed to contain short gaps between the 3′-OH end of the primer strand and the downstream 5′ phosphorylated DNA.[4,10,26] In order to probe structure−function properties of pol β when catalyzing replication on damaged DNAs, reactions were carried out on gapped and nongapped substrates in which the template nucleotide immediately downstream of the primer terminus was either (1) a dA (control) or (2) an exocyclic N^6-dA linked stereospecific polycyclic aromatic hydrocarbon, BPDE-adduct in either of two stereochemical orientations (−)-(7*S*,8*R*,9*S*,10*R*)-BPDE-dA ((−)-*anti-trans*-BPDE-dA) or (+)-(7*R*,8*S*,9*R*,10*S*)-BPDE-dA ((+)-*anti-trans*-BPDE-dA) (Figure 1A). The sequence context for the oligonucleotide design was the third position of

Table 1. Catalytic Efficiencies for Pol β Utilizing Major Groove Adducted BPDE-dA Adducted Templates

				discrimination		
template (dA)	incoming nucleotide	DNA gap	k_{cat}/K_m ($M^{-1}s^{-1}$)	f_{dNTP} [a]	f_{DNA} [b]	f_{adduct} [c]
unadducted	dTTP	−	0.68×10^6	1.0	1.0	1.0
	dATP	−	3.3	4.7×10^{-6}	1.0	
	dCTP	−	20.4	3.0×10^{-5}	1.0	
	dGTP	−	1.8	2.6×10^{-6}	1.0	
$C_{10}S$ BPDE	dTTP	−	4.9×10^2	1.0	1.0	1.4×10^3
	dATP	−	4.8	9.7×10^{-3}	1.0	
	dCTP	−	6.0	1.2×10^{-2}	1.0	
	dGTP	−	1.7	3.4×10^{-3}	1.0	
$C_{10}R$ BPDE	dTTP	−	29.1	1.0	1.0	2.3×10^4
	dATP	−	2.1	7.2×10^{-2}	1.0	
	dCTP	−	3.5	1.2×10^{-1}	1.0	
	dGTP	−	1.9	6.4×10^{-2}	1.0	
unadducted	dTTP	+	1.3×10^6	1.0	1.9	1.0
	dATP	+	3.9	3.0×10^{-6}	1.2	
	dCTP	+	35.8	2.7×10^{-5}	1.8	
	dGTP	+	2.3	1.7×10^{-6}	1.3	
$C_{10}S$ BPDE	dTTP	+	6.9×10^2	1.0	1.4	6.9×10^2
	dATP	+	10.4	1.5×10^{-1}	2.2	
	dCTP	+	9.7	1.4×10^{-2}	1.6	
	dGTP	+	3.0	4.4×10^{-3}	1.8	
$C_{10}R$ BPDE	dTTP	+	67.5	1.0	2.3	2.0×10^4
	dATP	+	8.5	1.3×10^{-1}	4.0	
	dCTP	+	3.6	5.4×10^{-2}	1.0	
	dGTP	+	2.1	3.2×10^{-2}	1.1	

[a] $f_{dNTP} = (k_{cat}/K_m)_{incorrect}/(k_{cat}/K_m)_{correct}$. [b] $f_{DNA} = (k_{cat}/K_m)_{gapped}/(k_{cat}/K_m)_{nongapped}$. [c] $f_{adduct} = (k_{cat}/K_m)_{unadducted}/(k_{cat}/K_m)_{adducted}$.

the N-*ras* codon 61 (CAA, where the underlined A is the position of the adduct) (Figure 2A). Although the site of adduction between these lesions and the nucleotide will position them in the major groove of the DNA, the potential biological consequences arising from the different orientations could be significant since the linkage at the C_{10} position of the BPDE adduct ($C_{10}S$ or $C_{10}R$) orients them to be pointing either toward or away from an oncoming DNA polymerase, respectively.[21]

Further, to determine the effects of positioning the same lesions in the DNA minor groove versus the major groove, chemically identical DNA adducts were linked through the exocyclic N^2-dG (Figure 1B). In this case, the sequence context was the human *N-ras* codon 12 (GGT, where the underlined G indicates the position of the adduct) (Figure 4A). As described above, the substrate DNAs position the control dG or modified nucleotides, (−)-(7*S*,8*R*,9*S*,10*R*)-BPDE-dG ((−)-*anti-trans*-BPDE-dG) or (+)-(7*R*,8*S*,9*R*,10*S*)-BPDE-dG ((+)-*anti-trans*-BPDE-dG), immediately downstream of the 3′-OH of the primer terminus. Similarly, the linkage at the C_{10} position of the BPDE adduct ($C_{10}S$ or $C_{10}R$) orients them to be pointing either toward or away from an oncoming DNA polymerase, respectively.[21] Thus, the experimental strategy was designed to test for how chemically similar but structurally distinct modifications can be used to probe structure−function relationships in pol β and the role that downstream DNA might play in the efficiency of insertion and extension reactions.

Pol β-Catalyzed TLS Past Major Groove-Linked BPDE Adducts. Using the template design depicted in Figure 2A, qualitative analyses of pol β-catalyzed primer extension reactions were evaluated over a range of dTTP concentrations, with and without two-nucleotide gapped DNA. As shown in Figure 2B, control reactions using an unadducted primer−template substrate revealed increases in both the processivity and efficiency of the gap-filling by pol β. This is well illustrated by comparing 5 and 15 min time points (odd and even lanes, respectively) with and without the downstream oligonucleotide (+ and −, respectively) with 100 nM dTTP concentration (Figure 2B, lanes 1−4) where in the absence of a DNA gap, the majority of DNA synthesis is a single nucleotide insertion with little or no extension. In contrast, in the presence of the downstream oligonucleotide, the majority of the products are filled two-nucleotide gaps. Qualitatively similar results were obtained over a range of dTTP concentrations (Figure 2B, lanes 5−16).

In contrast to that observed for the control substrates, when the templating nucleotide was the (+)-*anti-trans*-BPDE-dA in which the nucleotide linkage is 10*S* (pointing in the same direction as DNA synthesis) (Figure 2C), the presence of the downstream oligonucleotide becomes much more significant for the extension step following incorporation of dTTP opposite the lesion. As illustrated in lanes 1−4, at the lowest concentration of dTTP (100 μM), insertion was evident without a gapped substrate, but there were no detectable extension products (Figure 2C, lanes 1−2). However, when a downstream oligonucleotide was present creating a gapped DNA substrate, the majority of products resulted from complete gap-filling (i.e., two nucleotide insertions) (Figure 2C, + lanes). The effect of the gap on TLS was even more dramatic when the stereochemical orientation of the BPDE was reversed to the 10*R* orientation that is tilted toward the 3′ end of the template, in which the polymerase encounters greater hindrance to progression. This is evident in that even at the highest dTTP concentration (3.25 mM) very little extension could be detected (Figure 2D). Collectively, these data reveal that although the presence of these very bulky, major groove-linked lesions are significant blocks to

dx.doi.org/10.1021/tx300368f | *Chem. Res. Toxicol.* 2012, 25, 2744−2754

pol β DNA synthesis, the ability to catalyze extension reactions is highly dependent on the presence of downstream duplex DNA.

Following these qualitative analyses, the catalytic efficiencies for single-nucleotide insertion by pol β with control and the major groove-linked BPDE adducts were determined (Table 1). As previously reported, pol β displayed a very high discrimination for right versus wrong nucleotide insertion on the control substrate, with an ~2-fold increase in the catalytic efficiencies when the substrate containing a downstream oligonucleotide was used. When the $C_{10}S$ or $C_{10}R$ orientations of the BPDE-dA lesions were used as the templating nucleotides, insertion efficiencies were diminished significantly. Further, the discrimination between correct versus incorrect nucleotide insertion also decreased significantly, suggesting that pol β could be modestly error-prone if positioned to insert a nucleotide opposite a polycyclic aromatic hydrocarbon lesion. Even though the overall catalytic efficiencies were significantly reduced, the relative effect due to the presence or absence of the downstream primer was very similar to that observed for the control substrate, with the efficiencies increasing 2−4-fold in the presence of the primer.

The determination of the catalytic efficiencies described above relied on the incorporation of at least a single nucleotide; but in the sequence context used for these studies, these data capture both the insertion and extension steps and do not distinguish the relative efficiencies of these two processes. Since the qualitative data in Figure 2 suggested that there were large differences in the efficiencies of the extension steps, especially for the adducted templates, bypass efficiencies were calculated for each of the three substrates (Figure 3). Using the control substrate, the presence of the downstream oligonucleotide increased the bypass efficiency of the first insertion step by ~2.1-fold (Figure 3A). In contrast, when either of the BPDE-adducted substrates were used, although the incorporation of the second nucleotide was readily measured in the presence of the downstream oligonucleotide (triangles), in the absence of this DNA, the extension step dramatically reduced and never achieved the same level of extension efficiency, even at the highest dTTP concentrations (Figure 3B−C). Estimates of the increases in bypass for the $C_{10}S$ and $C_{10}R$ orientations of the BPDE-dA lesions were ~5- and 9-fold, respectively.

Pol β-Catalyzed TLS through Minor Groove-Linked BPDE Adducts. In order to access whether moving the position of the BPDE lesions from the major to the minor groove significantly altered the catalytic activity of pol β, primer−template duplexes were used as described in the Experimental Design section above (Figures 1B and 4A). In contrast to the data presented for pol β replication of the control adenine nucleotides, replication of the control guanine containing gapped substrate resulted in more inefficient dinucleotide incorporation when the downstream DNA was absent (11.5-fold, Table 2; Figure 5A). In contrast, in the absence of a downstream oligonucleotide, the majority of DNA synthesis was incorporation of a single nucleotide at low dCTP concentrations (Figure 4B).

However, TLS of both the substrates containing either the $C_{10}S$- or $C_{10}R$-BPDE-dG as the templating nucleotide was reduced by several orders of magnitude relative to the control dG, with single nucleotide incorporation opposite the lesion occurring both with and without the downstream oligonucleotide (Figure 4C and D, respectively). When the lesion was in the $C_{10}S$ orientation, the extension step was only evident when the gapped substrate was used (Figure 4C), while for the $C_{10}R$-containing substrate, the extension step was negligible, even on

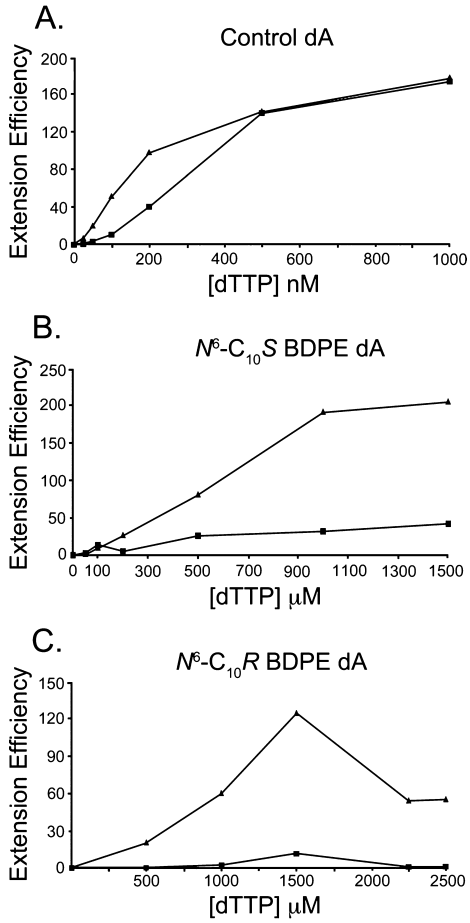

Figure 3. Influence of gapped DNA on the bypass of a major groove DNA lesion. (A) Replication on an unadducted template. The efficiency of bypass and measurement of incorporation beyond the control dA templating base was calculated at different dTTP concentrations in the absence or presence of a downstream strand (square and triangle symbols, respectively). Bypass efficiency was calculated as outlined in Experimental Procedures. All reactions included 10 fmol of pol β and were carried out for 5 min. (B) Bypass with a $C_{10}S$ BPDE-dA adducted template. (C) Bypass with a $C_{10}R$ BPDE-dA adducted template. Note that bypass efficiencies in the absence of a downstream oligonucleotide are so poor that those values do not reflect a full bypass.

the gapped substrate (Figure 4D). The catalytic efficiencies were determined only for dCTP incorporation because incorrect nucleoside incorporation was too inefficient to be accurately measured (Table 2). These data showed that pol β replication past the minor groove adducts was decreased 4−5 orders of magnitude compared to that in the control unadducted DNA. Although the presence of downstream DNA had a modest effect on the catalytic efficiencies with the lesion-containing substrates, the efficiency of the bypass step on the control guanine dinucleotide substrate was significantly elevated (11.5-fold, Table 2). This effect is clearly shown from calculations of the bypass efficiencies on control and adduct-containing substrates (Figure 5A−C). Unlike the control dA-extension reactions (Figure 3A), the bypass extension efficiency of the control dG nongapped DNA could not attain the same levels as that for the reactions carried out on the gapped substrate (Figure 5A). However, when the orientation of the BPDE adduct was pointed in the same direction as the polymerase (i.e., $C_{10}S$), there was a very large increase in the efficiency of the bypass step, with the increase in bypass estimated at ~10-fold (Figure 5B). A

dx.doi.org/10.1021/tx300368f | Chem. Res. Toxicol. 2012, 25, 2744−2754

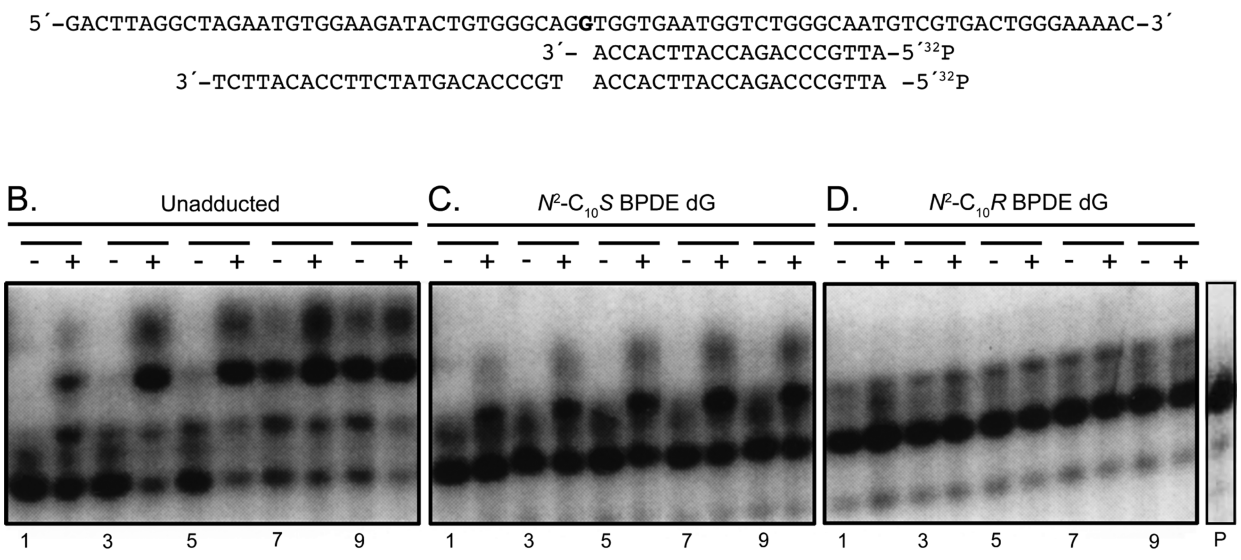

Figure 4. DNA pol β catalyzed DNA synthesis modulated by gapped DNA and a minor-groove BPDE-adduct. (A) Schematic of DNA substrates for DNA synthesis reactions. The bold **G** indicates the position of the unadducted $C_{10}S$ BPDE-dG or $C_{10}R$ BPDE-dG. The radio-labeled primer strand is indicated by the 5′-^{32}P label. (B) DNA synthesis reactions (15 min) using an unadducted template without (−) or with (+) a downstream unlabeled oligonucleotide strand. Lanes 1−2, 3−4, 5−6, 7−8, and 9−10 include pol β (10 fmol) with 0.5, 5, 10, 50, and 100 nM dCTP, respectively. (C) DNA synthesis reactions (15 min) using the $C_{10}S$ BPDE-dG adducted template without (−) or with (+) a downstream unlabeled oligonucleotide strand. Lanes 1−2, 3−4, 5−6, 7−8, and 9−10 include pol β (10 fmol) with 25, 50, 100, 200, and 500 μM, respectively. (D) DNA synthesis reactions (15 min) using the $C_{10}R$ BPDE-dG adducted template without (−) or with (+) a downstream unlabeled oligonucleotide strand. Lanes 1−2, 3−4, 5−6, 7−8, and 9−10 include pol β (10 fmol) with 100, 200, 500, 1000, and 1500 μM dCTP, respectively.

Table 2. Catalytic Efficiencies for dCTP Insertion with Pol β Utilizing Minor Groove Adducted BPDE-dG Adducted Templates

			discrimination	
template (dG)	DNA gap	k_{cat}/K_m ($M^{-1}s^{-1}$)	f_{DNA} [a]	f_{adduct} [b]
unadducted	−	7.2×10^6	1.0	1.0
$C_{10}S$ BPDE	−	4.8×10^2	1.0	1.5×10^4
$C_{10}R$ BPDE	−	1.0×10^2	1.0	7.2×10^4
unadducted	+	8.3×10^7	11.5	1.0
$C_{10}S$ BPDE	+	8.2×10^2	1.7	1.0×10^5
$C_{10}R$ BPDE	+	1.2×10^2	1.2	6.9×10^4

[a] $f_{DNA} = (k_{cat}/K_m)_{gapped}/(k_{cat}/K_m)_{nongapped}$. [b] $f_{adduct} = (k_{cat}/K_m)_{unadducted}/(k_{cat}/K_m)_{adducted}$.

comparable estimate for the $C_{10}R$-containing substrate is ∼4-fold; however, this value is derived from data in which pol β exhibited extremely poor incorporation efficiencies (Figure 5C).

TLS by Pol β Mutants. DNA pol β has been extensively analyzed by X-ray crystallographic and NMR spectroscopic methods, and numerous mutants have been characterized for their roles in various steps in the catalytic cycle.[1] Four pol β side chains that interact with the minor groove edge of the substrates (DNA and dNTP) have been substituted with alanine (K234A, Y271A, and N279A) or lysine (R283K). These mutants exhibit moderate or no loss in activity.[23] Arg283 interacts with the template strand in the closed active polymerase conformation and lysine substitution (R283K) results in an increase in base substitution and one-base deletion error rates.[13,27] In contrast, Asn279 hydrogen bonds to the minor groove edge of the base of the incoming nucleotide. Alanine substitution (N279A) results in a decrease in the error rates for base substitutions.[23,28] Lys234 and Tyr271 interact with the minor groove of the primer strand in the closed polymerase conformation. The substrate interactions of these residues are illustrated in Figure 6. The mutant enzymes were analyzed for their ability to catalyze TLS on the BPDE-adducted DNAs described above.

The catalytic efficiencies of each of these mutants were analyzed for the incorporation step on control and adducted DNAs with the lesions being in both the major and minor grooves (Tables 3 and 4). Analyses of these data reveal that there were very similar trends between the wild-type enzyme and each of the 4 mutants, with a significant reduction in the bypass efficiencies of TLS for all mutants tested when replicating DNAs containing adducts in either the major or the minor groove. Importantly, in all cases the severity of the blockage was more severe for the minor groove adducts relative to those in the major groove. Also, as described above for the wild-type enzyme, bypass efficiencies were calculated for each of the mutants using all three substrates (Figure 7). For all mutant enzymes, using the control or adducted substrate, the presence of the downstream oligonucleotide increased the efficiency of the bypass step, but in no cases were dTTP or dCTP concentrations high enough to overcome the effects of the downstream DNA.

Lys234 interacts in the minor groove upstream of the n-2 nucleotide in the primer strand (Figure 6). Thus, this residue monitors interactions in the duplex region near the primer terminus. Bypass of an adducted template would position the adduct opposite the primer terminus (i.e., insertion/translocation prior to extension). The catalytic efficiency with control substrates is similar to that of the wild-type enzyme (Tables 3 and 4). The bypass efficiency for the mutant is significantly diminished on unadducted templates but not the dA-adducted templates relative to wild-type enzyme. This suggests that K234 contributes key interactions during the DNA synthesis of unmodified substrates but that the adducts perturb the DNA substrate so that the importance of this interaction is masked

dx.doi.org/10.1021/tx300368f | Chem. Res. Toxicol. 2012, 25, 2744−2754

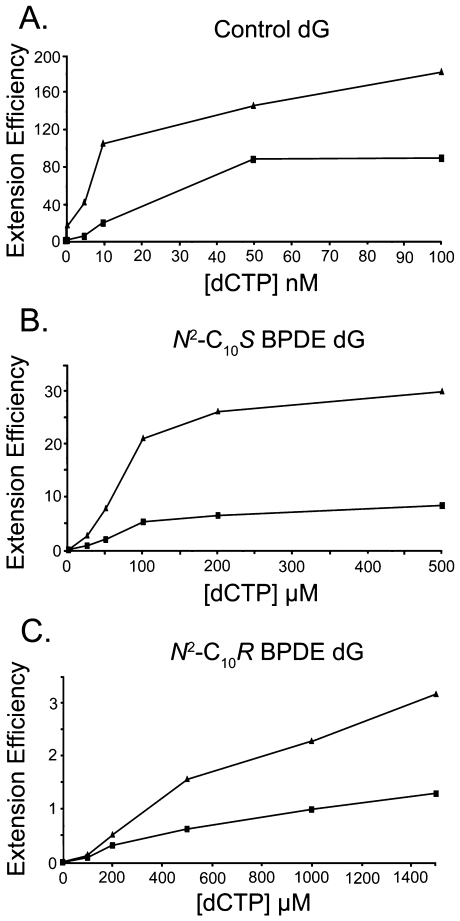

Figure 5. Influence of gapped DNA on bypass of a minor groove DNA lesion. (A) Replication on an unadducted template. The efficiency of bypass and the measurement of incorporation beyond the control dG templating base were calculated at different dCTP concentrations in the absence or presence of a downstream strand (square and triangle symbols, respectively). Bypass efficiency was calculated as outlined in Experimental Procedures. All reactions included 10 fmol of pol β and were carried out for 5 min. (B) Bypass with a $C_{10}S$ BPDE-dG adducted template. (C) Bypass with a $C_{10}R$ BPDE-dG adducted template. Note that bypass efficiencies in the absence of a downstream oligonucleotide are so poor that those values do not reflect a full bypass.

(i.e., decreased Lys234 minor groove interactions with adducted-dA).

While the ratios of the catalytic efficiencies (f_{DNA}) for the wild-type pol β for gapped DNA ranged from 1.39 for the major groove $C_{10}S$ to 3.27 for the equivalent $C_{10}R$, the mutant Y271A showed the greatest disparity in catalytic efficiencies, with 8.18 for the $C_{10}R$ to 17.04 for the equivalent $C_{10}S$. This is due to both a decrease in efficiency with nongapped DNA as well as an increase in efficiency for gapped DNA relative to wild-type enzyme. This side chain is situated in a polymerase subdomain that repositions itself upon binding a nucleotide. In the absence of a nucleotide, it interacts with the minor groove edge of the templating nucleotide but hydrogen bonds with the primer terminus subsequent to nucleotide binding.[29] Thus, the site of this mutation would be expected to interfere with subdomain motions, templating, and/or primer positioning.

As described above, the wild-type enzyme had a very significant difference in gap-filling when the dinucleotide was AA (1.9, Table 1) compared to GG (11.5, Table 2). This difference was not evident for the adducted DNAs. However, in

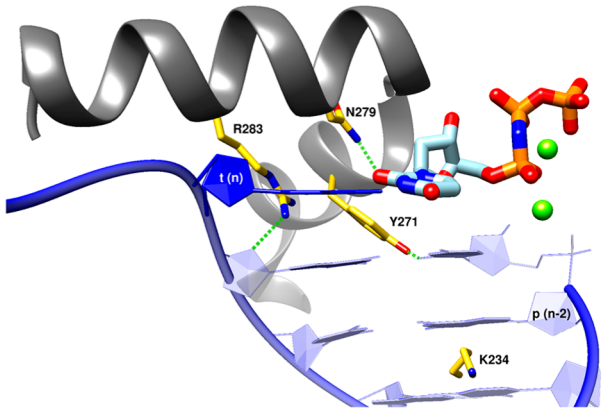

Figure 6. Nascent base pair binding pocket of DNA pol β. The side chains of residues Lys234 (K234), Asn279 (N279), Tyr271 (Y271), and Arg283 (R283) interact with the minor groove edge of the incoming nucleotide and DNA. These residues can hydrogen bond indiscriminately to the O2 of pyrimidines or the N3 of purines in the DNA minor groove. Arg283 and Asn279 hydrogen bond (green dashed lines) with the template strand (templating base is bark blue, t(n)) and incoming nucleotide (stick representation with light blue carbons), respectively. Tyr271 hydrogen bonds with the minor groove edge of the primer terminus, whereas Lys234 interacts with the minor groove upstream of the n-2 primer strand nucleotide. These residues are located in α-helices M and N (gray ribbons) in the N-subdomain that undergoes repositioning upon binding an incoming nucleoside triphosphate. The active site metals (Mg^{2+}) are illustrated as green spheres. This figure was created with Chimera.[34]

the case of the Y271A mutant, although gapped DNA discrimination was similar to that of the wild-type enzyme, a high degree of gapped DNA enhancement was also observed when the substrates were either of the $C_{10}S$ BPDE-adducts (dA and dG). This observation also extends to the $C_{10}R$ BPDE-dA substrate.

The gapped DNA and adduct discrimination for the N279A and R283K mutants were similar to those of the wild-type pol β (Tables 3 and 4). These residues interact with the incoming nucleotide and template strand, respectively (Figure 6). Although R283K exhibits lower catalytic efficiencies than the other mutants, discrimination and bypass (Figure 7) are similar to those of the other enzymes.

HIV-1 Reverse Transcriptase-Catalyzed TLS Past Major Groove-Linked BPDE Adducts. To test whether these findings with pol β also correctly predict the TLS capacities of additional DNA polymerases, further investigations were also performed using the HIV-1 reverse transcriptase (RT). Both of the stereoisomers of the N^6-BPDE-dA adducts were used and reactions carried out under single hit conditions with <30% primer extensions analyzed (Figure 8). As was the case for wild-type pol β, the BPDE-adducts posed a very significant block to polymerase progression, with catalytic efficiencies dropping nearly 5 orders of magnitude. The pattern of nucleotide discrimination opposite the lesions was similar to that observed for pol β, but the absolute catalytic efficiencies were significantly greater for this polymerase than the repair enzyme pol β.

DISCUSSION

Previously, pol β has been shown to catalyze synthesis past a variety of damaged DNAs, including abasic sites,[11] 8-oxo-dG,[12] benzo[*c*]phenanthrene diolepoxide adducts,[8] and cross-links formed from treatments with chemotherapeutic drugs such as

Table 3. Catalytic Efficiencies for dTTP Insertion for Wild-Type and Mutant Pol β Utilizing Major Groove BPDE-dA Adducted Templates

pol β	template (dA)	DNA Gap	k_{cat}/K_m ($M^{-1}s^{-1}$)	discrimination f_{DNA}[a]	discrimination f_{adduct}[b]
WT[c]	unadducted	−	3.7×10^5	1.0	1.0
	$C_{10}S$ BPDE	−	1.8×10^2	1.0	2.1×10^3
	$C_{10}R$ BPDE	−	2.0×10^1	1.0	1.8×10^4
	unadducted	+	5.9×10^5	1.60	1.0
	$C_{10}S$ BPDE	+	2.5×10^2	1.39	2.4×10^3
	$C_{10}R$ BPDE	+	6.6×10^1	3.27	8.9×10^3
K234A	unadducted	−	2.7×10^5	1.0	1.0
	$C_{10}S$ BPDE	−	1.4×10^2	1.0	1.9×10^3
	$C_{10}R$ BPDE	−	1.2×10^1	1.0	2.2×10^4
	unadducted	+	8.1×10^5	3.0	1.0
	$C_{10}S$ BPDE	+	4.0×10^2	2.86	2.0×10^3
	$C_{10}R$ BPDE	+	7.5×10^1	6.12	1.1×10^5
Y271A	unadducted	−	9.1×10^5	1.0	1.0
	$C_{10}S$ BPDE	−	2.7×10^1	1.0	3.4×10^4
	$C_{10}R$ BPDE	−	2.2×10^1	1.0	4.1×10^4
	unadducted	+	2.1×10^6	2.31	1.0
	$C_{10}S$ BPDE	+	4.6×10^2	17.04	4.6×10^3
	$C_{10}R$ BPDE	+	1.8×10^2	8.18	1.2×10^4
N279A	unadducted	−	3.8×10^5	1.0	1.0
	$C_{10}S$ BPDE	−	8.7×10^1	1.0	4.4×10^3
	$C_{10}R$ BPDE	−	1.0×10^1	1.0	3.8×10^4
	unadducted	+	5.1×10^5	1.34	1.0
	$C_{10}S$ BPDE	+	1.3×10^2	1.49	3.9×10^3
	$C_{10}R$ BPDE	+	2.0×10^1	2.0	2.6×10^4
R283K	unadducted	−	2.2×10^4	1.0	1.0
	$C_{10}S$ BPDE	−	1.1×10^1	1.0	2.0×10^3
	$C_{10}R$ BPDE	−	6.4	1.0	3.4×10^3
	unadducted	+	4.2×10^4	1.91	1.0
	$C_{10}S$ BPDE	+	1.6×10^1	1.46	2.6×10^3
	$C_{10}R$ BPDE	+	1.2×10^1	1.88	3.5×10^3

[a] $f_{DNA} = (k_{cat}/K_m)_{gapped}/(k_{cat}/K_m)_{nongapped}$. [b] $f_{adduct} = (k_{cat}/K_m)_{unadducted}/(k_{cat}/K_m)_{adducted}$. [c] Wild-type enzyme.

Table 4. Catalytic Efficiencies for dCTP Insertion with Wild-Type and Mutant Pol β Utilizing Minor Groove BPDE-dG Adducted Templates

pol β	template (dG)	DNA gap	k_{cat}/K_m ($M^{-1}s^{-1}$)	discrimination f_{DNA}[a]	discrimination f_{adduct}[b]
WT[c]	unadducted	−	7.2×10^6	1.0	1.0
	$C_{10}S$ BPDE	−	4.8×10^2	1.0	1.5×10^4
	$C_{10}R$ BPDE	−	1.0×10^2	1.0	7.2×10^4
	unadducted	+	8.3×10^7	11.5	1.0
	$C_{10}S$ BPDE	+	8.2×10^2	1.7	1.0×10^5
	$C_{10}R$ BPDE	+	1.2×10^2	1.2	6.9×10^5
K234A	unadducted	−	2.4×10^6	1.0	1.0
	$C_{10}S$ BPDE	−	3.5×10^2	1.0	6.9×10^3
	$C_{10}R$ BPDE	−	8.3×10^1	1.0	2.9×10^4
	unadducted	+	2.0×10^7	8.3	1.0
	$C_{10}S$ BPDE	+	4.1×10^2	1.2	4.9×10^4
	$C_{10}R$ BPDE	+	3.9×10^2	4.7	5.1×10^4
Y271A	unadducted	−	1.7×10^6	1.0	1.0
	$C_{10}S$ BPDE	−	1.9×10^2	1.0	8.9×10^3
	$C_{10}R$ BPDE	−	9.6×10^1	1.0	1.8×10^4
	unadducted	+	1.7×10^6	10.0	1.0
	$C_{10}S$ BPDE	+	2.1×10^3	11.1	8.1×10^2
	$C_{10}R$ BPDE	+	6.7×10^1	0.7	2.5×10^4
N279A	unadducted	−	5.8×10^6	1.0	1.0
	$C_{10}S$ BPDE	−	4.7×10^2	1.0	1.2×10^4
	$C_{10}R$ BPDE	−	3.2×10^1	1.0	1.8×10^5
	unadducted	+	2.1×10^7	3.6	1.0
	$C_{10}S$ BPDE	+	1.0×10^3	2.1	2.1×10^4
	$C_{10}R$ BPDE	+	4.9×10^1	1.5	4.3×10^4
R283K	unadducted	−	6.4×10^5	1.0	1.0
	$C_{10}S$ BPDE	−	2.3×10^2	1.0	2.8×10^3
	$C_{10}R$ BPDE	−	1.1×10^1	1.0	5.8×10^4
	unadducted	+	1.8×10^6	2.8	1.0
	$C_{10}S$ BPDE	+	9.0×10^2	3.9	2.0×10^3
	$C_{10}R$ BPDE	+	2.1×10^1	1.4	8.6×10^4

[a] $f_{DNA} = (k_{cat}/K_m)_{gapped}/(k_{cat}/K_m)_{nongapped}$. [b] $f_{adduct} = (k_{cat}/K_m)_{unadducted}/(k_{cat}/K_m)_{adducted}$. [c] Wild-type enzyme.

cisplatin.[10] In contrast, prior investigations using BPDE-adducted DNAs revealed that even under multiple hit conditions pol β terminated one nucleotide 3′ to the N^6 adenine $C_{10}R$-BPDE adduct and opposite the $C_{10}S$-BPDE adduct, with nucleotide incorporation opposite both these BPDE-adducted sites being predominantly T, followed to a much lesser extent by A > G opposite the $C_{10}R$-adducts and A > C>G opposite the $C_{10}S$-adducts.[21] These data suggested that under simple primer extension conditions, pol β could not play a significant role in TLS of these lesions. The design of the current investigation was to determine whether the efficiency and fidelity of TLS by pol β could be modulated in the context of a gapped substrate in which the downstream DNA was positioned appropriately for interaction with the flexible amino-terminal 8 kDa domain. This domain has deoxyribose phosphate lyase activity that removes a sugar−phosphate intermediate during BER.[30] Subsequently, the 8 kDa domain binds avidly to the 5′-phosphate in the gapped substrate.[4] The current investigations were designed to interrogate whether chemically identical lesions that differed only in their stereospecificity of the base linkage or the location of the site of attachment (minor or major groove) would affect TLS. Additionally, the roles that specific residues in pol β play in modulating the efficiencies of TLS were studied by analyzing four mutant enzymes of pol β that interact with the minor groove edge of the DNA (i.e., K234A, Y271A, and R283K) or incoming dNTP (i.e., N279A). Collectively, the findings presented herein showed that under reaction conditions in which pol β-catalyzed dinucleotide polymerization reactions were carried out, (1) the presence of any of the BPDE adducts significantly decreased insertion and bypass efficiency but generally not the fidelity of incorporation opposite the adduct (Figures 2−5), (2) the effect of the stereospecific orientation of the adducts showed that the lesions that were more blocking occurred when the lesion was pointed toward the oncoming polymerase rather than in the same direction of polymerization (Figures 2 and 4), (3) the adducts that were linked through the minor groove site were much more inhibitory to polymerization than those in the major groove (Figures 2 and 4; Tables 2 and 3), (4) the efficiency of the bypass reaction was highly dependent on the presence of a downstream DNA molecule (Figures 3 and 5), and (5) specific interactions of pol β with its substrates play critical roles in the efficiencies of these TLS reactions, as revealed by analyses of specific mutant polymerases (Tables 3 and 4).

Concerning a subset of the pol β mutants, the R283K mutant has been shown to exhibit a modestly reduced efficiency with a concomitant loss in fidelity.[23] Recent structural characterization

dx.doi.org/10.1021/tx300368f | Chem. Res. Toxicol. 2012, 25, 2744−2754

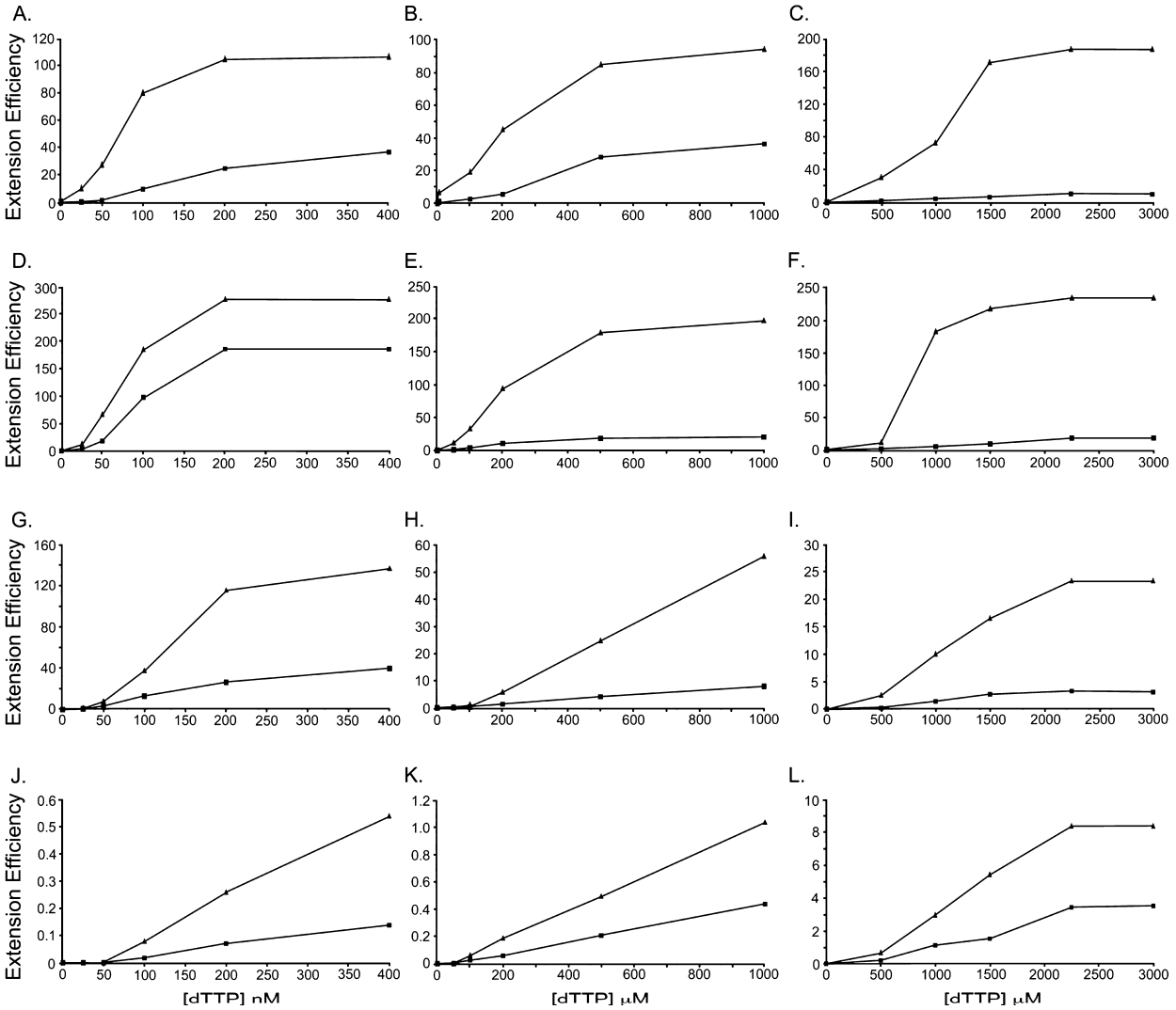

Figure 7. Influence of gapped DNA on the bypass of a major groove DNA lesion with mutants of pol β. Replication on an unadducted template with K234A, Y271A, N279A, and R283K, (panels A, D, G, and J, respectively). The efficiencies of bypass and measurement of incorporation beyond the control dA templating base were calculated at different dTTP concentrations in the absence or presence of a downstream strand (square and triangle symbols, respectively). Bypass efficiencies were calculated as outlined in Experimental Procedures. All reactions included 10 fmol of pol β and were carried out for 5 min. Bypass with a $C_{10}S$ BPDE-dA adducted template with K234A, Y271A, N279A, and R283K, (panels B, E, H, and K, respectively). Bypass with a $C_{10}R$ BPDE-dA adducted template with K234A, Y271A, N279A, and R283K, (panels C, F, I, and L, respectively).

of this mutant indicates that the enzyme favors an inactive open conformation upon correct nucleotide binding.[31] Additionally, the base substitution[27] and frameshift fidelities[13] of this mutant are decreased. This mutant exhibited a catalytic efficiency for bypassing the $C_{10}S$ BPDE-dA major groove adduct 50-fold less than that of the wild-type enzyme. In contrast, this mutant exhibited a bypass efficiency with the $C_{10}R$ BPDE-dG minor groove adduct only 2- times less than that of the wild-type enzyme suggesting that the conservative lysine substitution was tolerated in the minor groove but not in the major groove.

In contrast, N279A is known to interact with the incoming nucleotide and exhibits a higher fidelity than wild-type pol β.[23] This mutant had a bypass efficiency with the $C_{10}R$ BPDE-dG minor groove adduct that was significantly greater (13-fold) than that with wild-type pol β. Likewise, the mutant exhibited a bypass efficiency with the $C_{10}S$ BPDE-dA major groove adduct to be about 4.4-fold higher than that of the wild type. Thus, the results strongly demonstrate that in addition to the significant role of the stereospecificity, sequence context (*N-ras* codon dA-61[3] or dG-12[2]), and DNA position (minor or major groove) of these bulky adducts on bypass efficiency, the ability to bypass a lesion can be enhanced with gapped DNA and depends on specific polymerase interactions in the DNA minor groove.

To test whether these findings with a DNA repair polymerase such as pol β can be extrapolated to replicative polymerases, the TLS capacity of HIV-1 RT was analyzed. Our observations indicate that this processive polymerase can bypass both stereoisomers of the N^6 BPDE-dA adducts with limited encounters (i.e., under single hit conditions) (Figure 8). As was the case for wild-type pol β, these BPDE adducts posed very significant blocks to polymerase progression, with catalytic efficiencies dropping between 3 and 6 orders of magnitude. In addition, like wild-type pol β, correct dNTP was always preferentially incorporated. Since the following templating base was also adenine, insertion could be opposite the adduct or the downstream templating base. Interestingly, the pattern of misincorporation by HIV-1 RT was very similar to that of pol β. However, in contrast to pol β, the HIV-1 RT polymerase

dx.doi.org/10.1021/tx300368f | *Chem. Res. Toxicol.* 2012, 25, 2744−2754

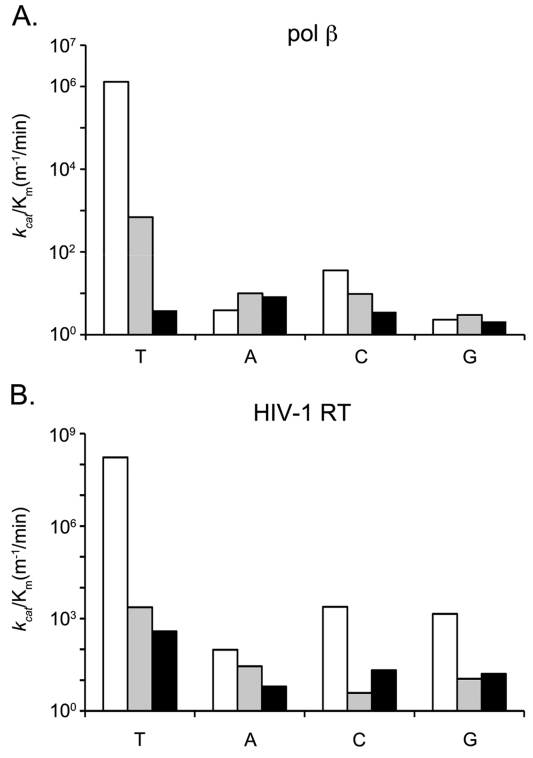

Figure 8. Effect of the major groove BPDE-dA adduct on RT insertion efficiencies. (A) Catalytic efficiencies for RT insertion with unadducted templates (open bar), $C_{10}S$-BPDE-dA (gray bar), and $C_{10}R$-BPDE-dA (black bar) adducted templates with alternate incoming nucleotides. (B) Similar histogram for pol β.

showed much higher catalytic efficiencies on the unadducted and BPDE-adducted templates as expected for a replicative polymerase.[32]

DNA polymerase β primarily interacts with DNA through sequence independent interactions (sugar−phosphate backbone and minor groove).[33] Like other members of the X-family of DNA polymerases, pol β is well suited to fill short gaps in DNA.[5] Generally, polymerases in the X-family exhibit low efficiency on nongapped DNA substrates resulting in distributive DNA synthesis. Thus, lesions in DNA are strong blocks to DNA synthesis. In contrast, the high affinity for gapped DNA through specific interactions with the 5′-margin of the gap targets the polymerase to gapped DNA. If a 3′-hydroxyl is nearby (i.e., short gap), then complete processive gap filling can occur. In this situation, the high affinity gap binding provides additional opportunities for the polymerase to bypass impediments in the template strand.

AUTHOR INFORMATION

Corresponding Author

*E-mail: lloydst@ohsu.edu.

Funding

This research was supported by NIH Grants P01 ES05355 and P01 CA160032 (to R.S.L.) and research project numbers Z01-ES050158 and Z01-ES050161 in the intramural research program of the NIH, National Institute of Environmental Health Sciences (to S.H.W.), and was in association with the National Institutes of Health Grant 1U19CA105010. Molecular graphics images were produced using the Chimera package[34] from the Resource for Biocomputing, Visualization, and Informatics at the University of California, San Francisco (supported by NIH P41 RR-01081).

Notes

The authors declare no competing financial interest.

ACKNOWLEDGMENTS

We are grateful to Drs. T. M. Harris and C. M. Harris for the syntheses and gift of the BPDE-adducted templates. We appreciate the assistance of Dan Austin in compiling and creating the figures. Special thanks go to Dr. Amanda K. McCullough for insightful comments on the manuscript.

ABBREVIATIONS

BPDE, 7,8-dihydrodiol-9,10-epoxides; pol, DNA polymerase; RT, HIV-1 reverse transcriptase; TLS, translesion DNA synthesis

REFERENCES

(1) Beard, W. A., and Wilson, S. H. (2006) Structure and mechanism of DNA polymerase *β*. *Chem. Rev. 106*, 361−382.

(2) Matsumoto, Y., and Kim, K. (1995) Excision of deoxyribose phosphate residues by DNA polymerase *β* during DNA repair. *Science 269*, 699−702.

(3) Piersen, C. E., Prasad, R., Wilson, S. H., and Lloyd, R. S. (1996) Evidence for an imino intermediate in the DNA polymerase *β* deoxyribose phosphate excision reaction. *J. Biol. Chem. 271*, 17811−17815.

(4) Prasad, R., Beard, W. A., and Wilson, S. H. (1994) Studies of gapped DNA substrate binding by mammalian DNA polymerase *β*: Dependence on 5′-phosphate group. *J. Biol. Chem. 269*, 18096−18101.

(5) Moon, A. F., Garcia-Diaz, M., Batra, V. K., Beard, W. A., Bebenek, K., Kunkel, T. A., Wilson, S. H., and Pedersen, L. C. (2007) The X family portrait: Structural insights into biological functions of X family polymerases. *DNA Repair 6*, 1709−1725.

(6) Canitrot, Y., Cazaux, C., Fréchet, M., Bouayadi, K., Lesca, C., Salles, B., and Hoffmann, J.-S. (1998) Overexpression of DNA polymerase *β* in cell results in a mutator phenotype and a decreased sensitivity to anticancer drugs. *Proc. Natl. Acad. Sci. U.S.A. 95*, 12586−12590.

(7) Servant, L., Cazaux, C., Bieth, A., Iwai, S., Hanaoka, F., and Hoffmann, J.-S. (2002) A role for DNA polymerase *β* in mutagenic UV lesion bypass. *J. Biol. Chem. 277*, 50046−50053.

(8) Batra, V. K., Shock, D. D., Prasad, R., Beard, W. A., Hou, E. W., Pedersen, L. C., Sayer, J. M., Yagi, H., Kumar, S., Jerina, D. M., and Wilson, S. H. (2006) Structure of DNA polymerase *β* with a benzo[*c*]phenanthrene diol epoxide-adducted template exhibits mutagenic features. *Proc. Natl. Acad. Sci. U.S.A. 103*, 17231−17236.

(9) Hoffmann, J. S., Pillaire, M. J., Garciaestefania, D., Lapalu, S., and Villani, G. (1996) *In vitro* bypass replication of the cisplatin-d(GpG) lesion by calf thymus DNA polymerase *β* and human immunodeficiency virus type I reverse transcriptase is highly mutagenic. *J. Biol. Chem. 271*, 15386−15392.

(10) Vaisman, A., and Chaney, S. G. (2000) The efficiency and fidelity of translesion synthesis past cisplatin and oxaliplatin GpG adducts by human DNA polymerase *β*. *J. Biol. Chem. 275*, 13017−13025.

(11) Efrati, E., Tocco, G., Eritja, R., Wilson, S. H., and Goodman, M. F. (1997) Abasic translesion synthesis by DNA polymerase *β* violates the "A-rule": Novel types of nucleotide incorporation by human DNA polymerase ß at an abasic lesion in different sequence contexts. *J. Biol. Chem. 272*, 2559−2569.

(12) Efrati, E., Tocco, G., Eritja, R., Wilson, S. H., and Goodman, M. F. (1999) "Action-at-a-distance" mutagenesis: 8-Oxo-7,8-dihydro-2′-deoxyguanosine causes base substitution errors at neighboring template sites when copied by DNA polymerase *β*. *J. Biol. Chem. 274*, 15920−15926.

(13) Osheroff, W. P., Beard, W. A., Yin, S., Wilson, S. H., and Kunkel, T. A. (2000) Minor groove interactions at the DNA polymerase *β* active

site modulate single-base deletion error rates. *J. Biol. Chem. 275*, 28033−28038.
(14) Batra, V. K., Beard, W. A., Shock, D. D., Pedersen, L. C., and Wilson, S. H. (2008) Structures of DNA polymerase β with active site mismatches suggest a transient abasic site intermediate during misincorporation. *Mol. Cell 30*, 315−324.
(15) Belousova, E. A., Maga, G., Fan, Y., Kubareva, E. A., Romanova, E. A., Lebedeva, N. A., Oretskaya, T. S., and Lavrik, O. I. (2010) DNA polymerases beta and lambda bypass thymine glycol in gapped DNA structures. *Biochemistry 49*, 4695−4704.
(16) Maga, G., Crespan, E., Wimmer, U., van Loon, B., Amoroso, A., Mondello, C., Belgiovine, C., Ferrari, E., Locatelli, G., Villani, G., and Hubscher, U. (2008) Replication protein A and proliferating cell nuclear antigen coordinate DNA polymerase selection in 8-oxo-guanine repair. *Proc. Natl. Acad. Sci. U.S.A. 105*, 20689−20694.
(17) Brown, W. C., and Romano, L. J. (1991) Effects of benzo[*a*]-pyrene-DNA adducts on a reconstituted replication system. *Biochemistry 30*, 1342−1350.
(18) Moore, P. D., Bose, K. K., Rabkin, S. D., and Strauss, B. S. (1981) Sites of termination of in vitro DNA synthesis on ultraviolet- and N-acetylaminofluorene-treated phi X174 templates by prokaryotic and eukaryotic DNA polymerases. *Proc. Natl. Acad. Sci. U.S.A. 78*, 110−114.
(19) Perlow, R. A., Kolbanovskii, A., Hingerty, B. E., Geacintov, N. E., Broyde, S., and Scicchitano, D. A. (2002) DNA adducts from a tumorigenic metabolite of benzo[a]pyrene block human RNA polymerase II elongation in a sequence- and stereochemistry-dependent manner. *J. Mol. Biol. 321*, 29−47.
(20) Jerina, D. M., Chadha, A., Cheh, A. M., Schurdak, M. E., Wood, A. W., and Sayer, J. M. (1991) Covalent bonding of bay-region diol epoxides to nucleic acids. *Adv. Exp. Med. Biol. 283*, 533−553.
(21) Chary, P., and Lioyd, S. (1995) *In vitro* replication by prokaryotic and eukaryotic polymerases on DNA templates containing site-specific and stereospecific benzo [*a*]pyrene-7, 8-dihydrodiol-9, 10-epoxide adducts. *Nucleic Acids Res. 23*, 1398−1405.
(22) Becerra, S. P., Kumar, A., Lewis, M. S., Widen, S. G., Abbotts, J., Karawya, E. M., Hughes, S. H., Shiloach, J., and Wilson, S. H. (1991) Protein-protein interactions of HIV-1 reverse transcriptase: Implication of central and C-terminal regions in subunit binding. *Biochemistry 30*, 11707−11719.
(23) Beard, W. A., Osheroff, W. P., Prasad, R., Sawaya, M. R., Jaju, M., Wood, T. G., Kraut, J., Kunkel, T. A., and Wilson, S. H. (1996) Enzyme-DNA interactions required for efficient nucleotide incorporation and discrimination in human DNA polymerase β. *J. Biol. Chem. 271*, 12141−12144.
(24) Harris, C. M., Zhou, L., Strand, E. A., and Harris, T. M. (1991) New strategy for the synthesis of oligodeoxynucleotides bearing adducts at exocyclic amino sites of purine nucleosides. *J. Am. Chem. Soc. 113*, 4328−4329.
(25) Kim, S. J., Stone, M. P., Harris, C. M., and Harris, T. M. (1992) A postoligomerization synthesis of oligodeoxynucleotides containing polycyclic aromatic hydrocarbon adducts at the N6 position of deoxyadenosine. *J. Am. Chem. Soc. 114*, 5480−5481.
(26) Singhal, R. K., and Wilson, S. H. (1993) Short gap-filling synthesis by DNA polymerase β is processive. *J. Biol. Chem. 268*, 15906−15911.
(27) Osheroff, W. P., Beard, W. A., Wilson, S. H., and Kunkel, T. A. (1999) Base substitution specificity of DNA polymerase β depends on interactions in the DNA minor groove. *J. Biol. Chem. 274*, 20749−20752.
(28) Miller, H., Prasad, R., Wilson, S. H., Johnson, F., and Grollman, A. P. (2000) 8-OxodGTP incorporation by DNA polymerase β is modified by active-site residue Asn279. *Biochemistry 39*, 1029−1033.
(29) Sawaya, M. R., Prasad, P., Wilson, S. H., Kraut, J., and Pelletier, H. (1997) Crystal structures of human DNA polymerase β complexed with gapped and nicked DNA: Evidence for an induced fit mechanism. *Biochemistry 36*, 11205−11215.
(30) Prasad, R., Shock, D. D., Beard, W. A., and Wilson, S. H. (2010) Substrate channeling in mammalian base excision repair pathways: Passing the baton. *J. Biol. Chem. 285*, 40479−40488.
(31) Freudenthal, B. D., Beard, W. A., and Wilson, S. H. (2012) Structures of dNTP intermediate states during DNA polymerase active site assembly. *Structure (Cambridge, MA, U. S.)*,.
(32) Beard, W. A., Shock, D. D., Vande Berg, B. J., and Wilson, S. H. (2002) Efficiency of correct nucleotide insertion governs DNA polymerase fidelity. *J. Biol. Chem. 277*, 47393−47398.
(33) Beard, W. A., and Wilson, S. H. (2000) Structural design of a eukaryotic DNA repair polymerase: DNA polymerase β. *Mutat. Res. 460*, 231−244.
(34) Pettersen, E. F., Goddard, T. D., Huang, C. C., Couch, G. S., Greenblatt, D. M., Meng, E. C., and Ferrin, T. E. (2004) UCSF Chimera: A visualization system for exploratory research and analysis. *J. Comput. Chem. 25*, 1605−1612.